Insect Biochemistry and Molecular Biology 104 (2019) 58–64

Contents lists available at ScienceDirect

Insect Biochemistry and Molecular Biology

journal homepage: www.elsevier.com/locate/ibmb

Function and pharmacology of glutamate-gated chloride channel exon 9 splice variants from the diamondback moth *Plutella xylostella*

Xingliang Wang[a], Andrias O. O´Reilly[b], Martin S. Williamson[c], Alin M. Puinean[d], Yihua Yang[a], Shuwen Wu[a], Yidong Wu[a,*]

[a] College of Plant Protection, Nanjing Agricultural University, Nanjing, China
[b] School of Natural Sciences and Psychology, Liverpool John Moores University, Liverpool, UK
[c] Biointeractions and Crop Protection Department, Rothamsted Research, Harpenden, UK
[d] Oxitec Limited, 71 Innovation Drive, Abingdon, Oxfordshire, UK

ARTICLE INFO

Keywords:
Glutamate-gated chloride channel
Alternative splicing
Abamectin
Fipronil
Diamondback moth

ABSTRACT

Glutamate-gated chloride channels (GluCls) are found only in invertebrates and mediate fast inhibitory neurotransmission. The structural and functional diversity of GluCls are produced through assembly of multiple subunits and via posttranscriptional alternations. Alternative splicing is the most common way to achieve this in insect GluCls and splicing occurs primarily at exons 3 and 9. As expression pattern and pharmacological properties of exon 9 alternative splices in invertebrate GluCls remain poorly understood, the cDNAs encoding three alternative splice variants (9a, 9b and 9c) of the PxGluCl gene from the diamondback moth *Plutella xylostella* were constructed and their pharmacological characterizations were examined using electrophysiological studies. Alternative splicing of exon 9 had little to no impact on PxGluCl sensitivity towards the agonist glutamate when subunits were singly or co-expressed in *Xenopus* oocytes. In contrast, the allosteric modulator abamectin and the chloride channel blocker fipronil had differing effects on PxGluCl splice variants. PxGluCl9c channels were more resistant to abamectin and PxGluCl9b channels were more sensitive to fipronil than other homomeric channels. In addition, heteromeric channels containing different splice variants showed similar sensitivity to abamectin (except for 9c) and reduced sensitivity to fipronil than homomeric channels. These findings suggest that functionally indistinguishable but pharmacologically distinct GluCls could be formed in *P. xylostella* and that the upregulated constitutive expression of the specific variants may contribute to the evolution of insecticide resistance in *P. xylostella* and other arthropods.

1. Introduction

Chloride-conducting members of the cysteine loop ligand-gated ion channel (cys-loop LGIC) family play an important role in inhibitory synaptic transmission in the nervous systems of vertebrates and invertebrates. γ-aminobutyric acid (GABA)-gated chloride channels (GABACls) are extensively expressed in the nervous systems of arthropods and nematodes as well as in higher animals (Buckingham et al., 2005). In contrast, cys-loop glutamate-gated chloride channels (GluCls) are found only in invertebrates (Cull-Candy, 1976; Wolstenholme, 2010). GABACls and GluCls are molecular targets for macrocyclic lactone insecticides (avermectins), which can activate these receptors directly, potentiate the response to the binding of their respective neurotransmitter or antagonize the agonist-induced channel current (Fuse et al., 2016; Wolstenholme, 2012). Phenylpyrazoles (e.g. fipronil) mainly target GABA receptors (Buckingham et al., 2005), but fipronil also showed inhibitory effects on GluCls, which acts as a blocker of these two types of LGICs (Kita et al., 2014; Narahashi et al., 2010; Wu et al., 2017; Zhao et al., 2004).

Cys-loop LGICs assemble as pentamers and each subunit has four transmembrane segments (TM1-TM4), a large N-terminal section that forms the extracellular neurotransmitter-binding domain and a comparatively smaller intracellular domain comprised mainly of the TM3-TM4 linker. LGICs can form as homomers or heteromers and different subunit combinations can produce receptors with diverse structural, functional and pharmacological properties. Six genes encode GluCl subunits in the nematode *Caenorhabditis elegans* and mite *Tetranychus urticae* (Jones and Sattelle, 2008; Dermauw et al., 2012). In contrast,

* Corresponding author.
E-mail addresses: wxl@njau.edu.cn (X. Wang), a.o.oreilly@ljmu.ac.uk (A.O. O´Reilly), martin.williamson@rothamsted.ac.uk (M.S. Williamson), mirel.puinean@oxitec.com (A.M. Puinean), yhyang@njau.edu.cn (Y. Yang), swwu@njau.edu.cn (S. Wu), wyd@njau.edu.cn (Y. Wu).

https://doi.org/10.1016/j.ibmb.2018.12.005
Received 19 June 2018; Received in revised form 24 October 2018; Accepted 11 December 2018
Available online 11 December 2018
0965-1748/

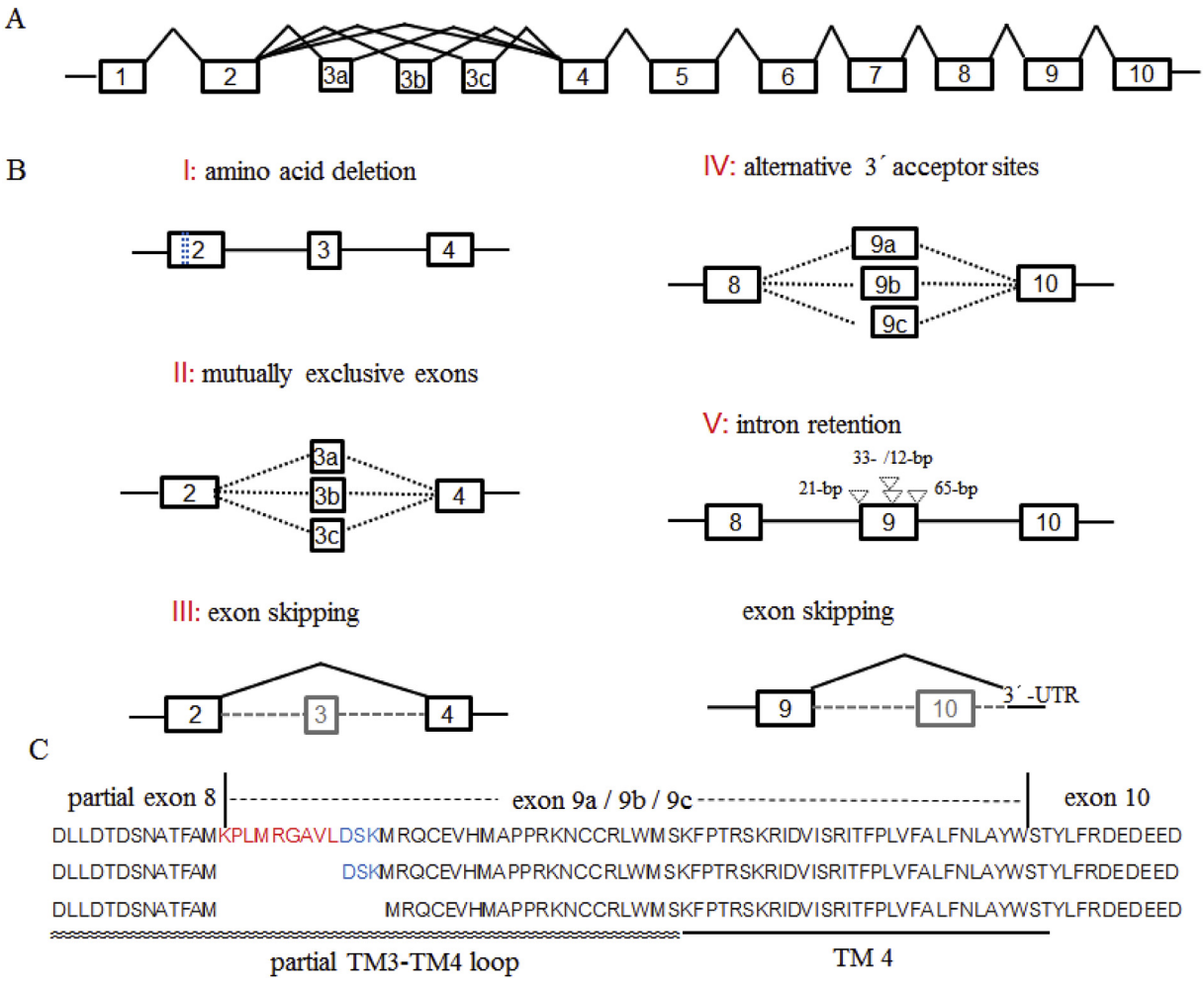

Fig. 1. Genomic structure and alternative splicing of the glutamate-gated chloride channel. (A) Typical genomic organization of GluCls. Exons are shown as boxes and introns as thin angled lines. (B) Reported alternative splice variants and amino acids deletion of GluCls. The deletion of four amino acids in exon 2 is indicated by blue dotted line and the insertions of partial introns are indicated by inverted triangles. (C) Sequence alignment of three PxGluCl splice variants: 9a (top), 9b (middle) and 9c (bottom). The partial TM3-TM4 loop and TM4 domains are indicated by wavy lines and a horizontal thick line, respectively. (For interpretation of the references to colour in this figure legend, the reader is referred to the Web version of this article.)

GluCls in insect species are encoded by a single gene. Studies on several species of Diptera, Hymenoptera, Coleoptera, Hemiptera show that subunit diversity arises from posttranscriptional alternations of mRNA i.e. from splice variants and RNA editing (Furutani et al., 2014; Jones et al., 2010; Jones and Sattelle, 2006; Kita et al., 2014; Meyers et al., 2015; Semenov and Pak, 1999; Wang et al., 2016a; Wu et al., 2017). An invertebrate GluCl gene consists typically of 10 exons (Fig. 1A) and an overview of the five different processes that produce different subunit variants is shown in Fig. 1B. In particular, exons 3 and 9 have been identified as “hot spot” domains of alternative splicing (Fig. 1B).

Exon 3 encodes a section of the extracellular ligand-binding domain and two variants in the 5′ region were first identified in *Drosophila melanogaster* (Semenov and Pak, 1999). These variants were initially termed modules 1 and 2 and correspond to exons 3a and 3b, respectively. To date, exon 3 alternative splice variants have been reported for the following insect species: *Apis. mellifera* (Jones and Sattelle, 2006) and *Nasonia vitripennis* (Jones et al., 2010) have two alternatives whereas *Tribolium castaneum* (Jones and Sattelle, 2007), *Musca domestica* (Kita et al., 2014), *Bombyx mori* (Furutani et al., 2014), *Anopheles gambiae* (Meyers et al., 2015), *Plutella xylostella* (Wang et al., 2016a) and *Laodelphax striatellus* (Wu et al., 2017) have three alternatives. In addition, a fourth variant that lacks exon 3 was observed in *B. mori* (Furutani et al., 2014) and *P. xylostella* (our unpublished data).

Exon 9 encodes a section of the intracellular TM3-TM4 linker and, as with exon 3, variants in this region were also identified first in the *D. melanogaster* GluCl: a 12-bp stretch immediately downstream of an intron ending in AG results in four additional amino acids inserted before the predicted TM4 segment (Semenov and Pak, 1999). Similarly, a 21-bp stretch is found in the *L. striatellus* GluCl (Wu et al., 2017) and a 65-bp insertion is added downstream of the *P. xylostella* GluCl (PxGluCl) exon 9 (Liu et al., 2014). In addition, a 33-bp insertion that was previously predicted to be part of intron 9 was found in *A. gambiae* GluCl (Meyers et al., 2015) (which the author defined as an additional exon 10 but we suggest is an exon 9 insertion following multi-sequences alignment analysis). In our previous study, alternative splicing of PxGluCl mRNA was detected in exon 9, which have three variants (exon 9a, 9b, 9c) as shown in Fig. 1 (Wang et al., 2016a). A 36-bp deletion variant (exon 9c in our study) was observed in an abamectin-resistant *P. xylostella* strain (Liu et al., 2014) and a partial deletion of exon 9 termed 9pΔ (also corresponding to exon 9c in our study) was found in *B. mori* GluCl (Furutani et al., 2014). Additionally, one exon skipping variant in the C-terminal amino acids sequences of *B. mori* GluCl was also detected in the larva brain (Furutani et al., 2014), which lacks the tenth exon.

Exon 3 splice variants have been well characterized in terms of GluCl function, pharmacology and spatiotemporal expression patterns (Furutani et al., 2014; Kita et al., 2014; Meyers et al., 2015; Wu et al., 2017). In contrast, little is known about the physiological roles and pharmacology of GluCls with exon 9 splice variants in the nervous

system of any invertebrate. Therefore, in the present study we cloned and constructed the GluCl 9a, 9b and 9c splice variants from the diamondback moth *P. xylostella*, a notorious pest of cruciferous vegetables worldwide. The three variants were expressed in *Xenopus* oocytes (both individually and in combination) and their electrophysiological responses examined with the endogenous agonist glutamate, the allosteric modulator abamectin (avermectin B1a) and the channel blocker fipronil. Our results demonstrate that functionally indistinguishable but pharmacologically distinct channels can form from alternative splice variants and we suggest the constitutive expression of these variants might affect insecticide toxicity in the field.

2. Materials and methods

2.1. Chemicals

L-Glutamic acid (≧99%) and fipronil (97.9%) were purchased from Sigma-Aldrich (St. Louis, MO, USA). Abamectin (B1a = 91.5%) was a gift from Veyong bio-chemical (Shijiazhuang, Hebei, CN). All the restricted enzymes used in this study, including *Eco*RI, *Xba*I, and *Not*I were purchased from Thermo Fisher Scientific (Waltham, MA, USA).

2.2. Molecular cloning of PxGluCl splice variants

Total RNA of 4th-instar larvae from the *P. xylostella* susceptible Roth strain was extracted by using the SV Total RNA Isolation System Kit (Promega, Madison, WI, USA) according to the manufacturer's protocol. First-strand cDNA was synthesized from 1 μg total RNA using an oligo $(dT)_{15}$ primer and M-MLV reverse transcriptase (Promega). The cDNA of PxGluCl (isoform 9a) was cloned using PCR oligonucleotide primers PxGluCl_*Eco*RI_F and PxGluCl_*Xba*I_R (Table 1). This cDNA also provided the template for PxGluCl9b and PxGluCl9c PCR amplification using KAPA HiFi HotStart PCR Kit (KAPA Biosystems, USA) as follows. The upstream fragment of PxGluCl9b was amplified using primers PxGluCl_EcoRI_F and PxGluC_9b_R, and the downstream fragment of PxGluCl9b was amplified using primers PxGluC_9b_F and PxGluCl_XbaI_R (Table 1). Full-length PxGluCl9b was amplified by fusion PCR using the two fragments as the mixed template. Similarly, the full-length cDNA of PxGluCl9c was generated by the corresponding primers (Table 1). The amplified full-length cDNA of each PxGluCl exon 9 splice variant was inserted into the cloning vector pJET1.2/blunt (Thermo Fisher Scientific, USA). After confirmation of their sequences (Eurofins Genomics, Germany), each recombinant plasmid of PxGluCl variant was digested with *Eco*RI and *Xba*I and the product (gel-purified) was ligated into the *Eco*RI and *Xba*I sites of the pGH19 vector, a modified version of plasmid pGEMHE, which contains 5′- and 3′-untranslated *X. laevis*beta-globin gene regions, and the presence of the variants were reconfirmed by nucleotide sequencing.

2.3. cRNA synthesis and injection into Xenopus oocytes

Each PxGluCl variant was extracted using the GeneJET plasmid miniprep kit (Thermo Scientific). Plasmids were linearized with *Not*I, and capped RNAs were generated using the T7 mMessage mMachine Kit (Ambion, Life Technologies, Paisley, UK) according to the manufacturer's instructions. Synthesized cRNAs were recovered by precipitation with isopropanol, dissolved in nuclease-free water at a final concentration of 500 ng/μL and stored at −80 °C until use.

Mature healthy *X. laevis* oocytes (stage V–VI) were treated with collagenase (type IA; 2 mg/mL; Sigma, USA) in calcium-free Barth's solution (88 mM NaCl; 2.4 mM $NaHCO_3$; 15 mM Tris-HCl; 1 mM KCl; 0.82 mM $MgCl_2$) for about 25 min at room temperature, rinsed three times, and manually defolliculated before injection with cRNA. Oocytes were injected with 32.2 nL cRNA (25 ng/μL) into the cytoplasm by using a Drummond variable volume microinjector. Alternatively, the oocytes were injected with a mixture of cRNAs (0.805 ng) composed of equal amount of two or three variants. After injection, calcium-containing Barth's solution (0.77 mM $CaCl_2$) with antibiotics (100 units/mL penicillin, 100 μg/mL streptomycin, 4 μg/mL kanamycin and 50 μg/mL tetracycline) was used for oocyte incubation at 18 °C. Experiments were carried out 3–5 days after injection.

2.4. Two-electrode voltage-clamp recordings

Xenopus oocytes were held in a recording bath and continuously perfused with a Ringer's solution (115 mM NaCl, 2.5 mM KCl, 1.8 mM $CaCl_2$, 10 mM HEPES, pH 7.3). Two-electrode voltage clamp was used for recording whole-cell currents from the injected *Xenopus* oocytes. The glass capillary electrodes were filled with 3 M KCl and had a resistance of 0.5–1.5 MΩ. All the experiments were performed at 18–22 °C, and the induced inward currents were recorded with an OC-725C oocyte clamp (Warner Instruments, Hamden, CT, USA) at a holding potential of −60 mV. Data acquisition and analysis were carried out using iWorx 408 data acquisition system and LabScribe software (iWorx Systems, Inc. Dover, NH, USA). Glutamate was dissolved in Ringer's solution and applied to the oocytes for 3 s. After the glutamate perfusion, the oocytes were washed by Ringer's solution for 2 min to assess their reproducibility. Abamectin was first dissolved in DMSO (0.1 mM) and then diluted with Ringer's solution. The abamectin solution containing ≤0.1% DMSO was applied to oocytes for 15 s, and the oocytes were then washed for 3 min. For measuring response to abamectin, all oocytes were tested with one-shot application to avoid the carry-over effect from previous abamectin applications. The activated currents by abamectin applications were normalized to the saturating glutamate-induced current in the same oocyte. The chloride channel blocker fipronil was first dissolved in DMSO and then diluted with Ringer's solution (≤0.1% DMSO). 0.1 mM glutamate was first applied to oocytes 2–3 times to record a control response. After the last application of glutamate the oocytes were immediately perfused with fipronil for 2.5 min, and then three further applications of 0.1 mM glutamate were made. For measuring inhibition by fipronil, all oocytes were tested with one-shot application protocol. The inhibition percentage was calculated from the average of two minimum responses to glutamate during the perfusion of fipronil. The same protocol was used for all variant channels. Fifty percent effective concentrations (EC_{50}s), Hill coefficients (nHs), and 50% inhibitory concentrations (IC_{50}s) were obtained from dose-response curves that were analyzed by nonlinear regression analysis using GraphPad Prism 5.0 (GraphPad Software Inc., San Diego, CA, USA). Data were obtained from at least four oocytes from at least two frogs.

Table 1
Sequences of primers used in this study.

Primer	Purpose	Sequence (5′ to 3′)
PxGluCl_EcoRI_F	Full-length cDNA amplification and fusion PCR	CGGAATTCGGTTTGCTGAGTTGGAGAATGGACG
PxGluCl_XbaI_R	Full-length cDNA amplification and fusion PCR	GCTCTAGATGCCAGTGGAACGATGCTGATGC
PxGluC_9b_F	Amplify the downstream fragment of 9b variant	CTTCGCGATGGACTCCAAGATGCGACAGTG
PxGluC_9b_R	Amplify the upstream fragment of 9b variant	TCTTGGAGTCCATCGCGAAGGTGGCATTG
PxGluC_9c_F	Amplify the downstream fragment of 9c variant	TTCGCGATGATGCGACAGTGCGAGGTG
PxGluC_9c_R	Amplify the upstream fragment of 9c variant	CACTGTCGCATCATCGCGAAGGTGGCATTG

2.5. Statistics

Data are given as means ± SEM. Statistical analysis was determined by a one-way ANOVA multiple comparison test or Student's *t*-test. Significance was set up at alpha = 0.05.

3. Results

3.1. Molecular cloning of PxGluCl splice variants

The full-length cDNA of PxGluCl3c9a was amplified from the susceptible Roth *P. xylostella* strain then subcloned and sequenced in our previous work (Wang et al., 2016a). This transcript (GenBank accession no. JX014231.1, referred to as '9a' in this study) consists of 1347-bp nucleotides that encode a protein of 448 amino acids. Two naturally occurring splice variants: PxGluCl9b and PxGluCl9c (referred to as 9b and 9c in this study, respectively) were also reported in Wang et al. (2016a). In the present study a high-fidelity fusion PCR strategy, using the 9a cDNA as template, the 9b and 9c splice variants were successfully amplified and confirmed by nucleotide sequencing (GenBank accession nos. MH459002 and MH459003). The translated protein sequences show that 9b and 9c have a loss of 9 and 12 amino acids, respectively, at the alternative 3′ acceptor site of exon 9, which encodes a part of the TM3-TM4 intracellular loop (Fig. 1C). To generate expression plasmids for electrophysiological studies, each of the three PxGluCl splice variants was subcloned into the pGH19 vector and verified by nucleotide sequencing.

3.2. Sensitivity of PxGluCl splice variants to glutamate

The alternatively spliced PxGluCl constructs 9a, 9b and 9c were expressed individually in *X. laevis* oocytes and the glutamate responses of these homomeric channels were recorded by two-electrode voltage-clamp technique. Glutamate concentration-response curves (C-R curves) were measured by applying concentrations ranging from 0.3 μM to 1 mM for each construct (see the sample traces shown in Fig. 2A). The application of glutamate to the three channels induced robust concentration-dependent inward currents, demonstrating that functional homomers can be formed by all splice variants. Meanwhile, application of glutamate in the same concentration range to control oocytes showed no response (data not shown). The C-R curves for 9a, 9b and 9c channels gave EC_{50}s of 17.70 ± 3.73 μM, 19.04 ± 1.99 μM and 21.89 ± 3.24 μM, respectively (Table 2, Fig. 2B). No significant differences were observed in the EC_{50}s and nHs among the three splice variants expressed singly in oocytes ($p > 0.05$).

As it is possible that heteromeric PxGluCls may assemble *in vivo* in *P. xylostella*, we measured the glutamate responses from oocytes co-injected with two or three different cRNAs. Glutamate C-R curve was generated from concentrations ranging from 0.1 μM to 0.1 mM for each construct. The C-R curves gave EC_{50}s of 8.21 ± 0.95 μM for 9a + 9b, 9.54 ± 1.67 μM for 9a + 9c, 15.83 ± 1.19 μM for 9b + 9c and 13.57 ± 1.20 μM for 9a + 9b + 9c channels (Table 2, Fig. 2C). When compared with co-expressed 9b + 9c channels, the potencies of glutamate in 9a + 9b and 9a + 9c heteromeric expressions were increased by 1.9- and 1.7-fold, respectively, significant differences in EC_{50}s were observed ($p < 0.05$), and reduction in nHs of 9a + 9b was also significant (Dunnett's Multiple Comparison Test, $p < 0.05$). Meanwhile, the Hill coefficient of 9b + 9c and 9a + 9b + 9c were 2.2 ± 0.39 (n = 9), 2.20 ± 0.31 (n = 8), respectively, suggesting that more than one glutamate molecule is required to activate these two co-expressed channels.

3.3. Sensitivity of PxGluCl splice variants to abamectin

The allosteric activator abamectin induced robust, slowly activating and irreversible currents (see the sample traces in Fig. 3A) for all

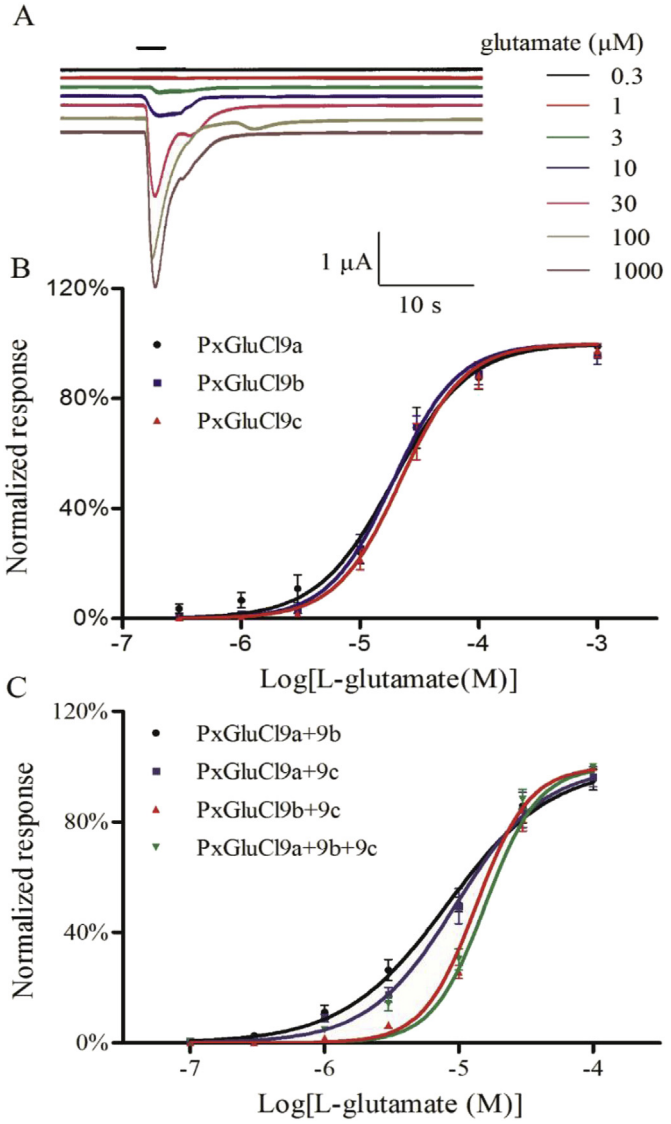

Fig. 2. Glutamate responses of *PxGluCls* containing variant subunits singly or co-expressed in *Xenopus* oocytes. (A) Representative current traces induced by glutamate from 0.3 μM to 1 mM in channels containing singly expressed 9a variant. (B) Glutamate concentration response curves from singly expressed variants. (C) Glutamate concentration response curves from co-expressed variants. Data are the mean ± SEM from n = 6–9 oocytes from 2 to 3 different frogs.

channels in a concentration-dependent fashion (Fig. 3). As shown in the Table 2, the EC_{50}s of abamectin calculated from C-R curves of singly expressed 9a, 9b and 9c channels were 0.13 ± 0.04 μM, 0.28 ± 0.12 μM and 1.07 ± 0.78 μM, respectively (Fig. 3B). When compared with 9a channels, 9b appeared less sensitive to abamectin with a 2.2-fold increase in EC_{50} but this difference was not significant ($p > 0.05$). In contrast, singly injected 9c oocytes showed significant reduction in sensitivity to abamectin. The EC_{50} of 9c was increased by 8.2-fold, and the nH of 9c was reduced by 3.7-fold. Both of the changes in EC_{50} and nH were significantly (Dunnett's Multiple Comparison Test, $p < 0.05$), which suggests that the absence of 12 amino acids in the TM3-TM4 loop of 9c channels results in abamectin insensitivity at the receptor level.

We also examined abamectin responses on the PxGluCl variants co-expressed in oocytes. The C-R curves gave EC_{50}s of 0.18 ± 0.09 μM for 9a + 9b, 0.20 ± 0.11 μM for 9a + 9c, 0.23 ± 0.15 μM for 9b + 9c and 0.32 ± 0.26 μM for 9a + 9b + 9c channels (Table 2, Fig. 3C). Abamectin activated each co-expressed channel with a similar EC_{50} and the

Table 2
Effects of glutamate and abamectin on membrane currents, and the effects of fipronil on glutamate-induced membrane currents from *Xenopus* oocytes containing variant subunits singly or co-expressed *PxGluCls*, with EC_{50} and IC_{50} values shown. Data are the mean ± SEM from n = 4–9 oocytes from 2 to 3 different frogs.

Variants	L-glutamate			Abamectin			Fipronil		
	n	EC_{50} μM	n_H	n	EC_{50} μM	n_H	n	IC_{50} μM	n_H
Singly expressed									
Exon 9a	7	17.70 ± 3.73	1.21 ± 0.37	7	0.13 ± 0.04	1.29 ± 0.08	5	10.22 ± 4.08	0.56 ± 0.09
Exon 9b	6	19.04 ± 1.99	1.60 ± 0.19	5	0.28 ± 0.12	0.60 ± 1.16	5	3.787 ± 2.02	0.48 ± 0.03
Exon 9c	6	21.89 ± 3.24	1.60 ± 0.22	5	1.07 ± 0.78[b]	0.35 ± 0.02	6	12.92 ± 7.65	0.43 ± 0.07
Co-expressed									
Exon 9a + 9b	6	8.21 ± 0.95[a]	1.12 ± 0.21	5	0.18 ± 0.09	0.99 ± 0.07	5	55.45 ± 19.48	0.50 ± 0.12
Exon 9a + 9c	6	9.54 ± 1.67[a]	1.33 ± 0.10	5	0.20 ± 0.11	1.03 ± 0.09	4	32.67 ± 21.09	0.45 ± 0.03
Exon 9b + 9c	9	15.83 ± 1.19	2.20 ± 0.39	4	0.23 ± 0.15	1.07 ± 0.15	5	16.47 ± 6.92	0.31 ± 0.04
Exon 9a + 9b + 9c	8	13.57 ± 1.20	2.20 ± 0.31	5	0.32 ± 0.26	0.58 ± 0.11	4	57.99 ± 14.55	0.49 ± 0.09

[a] Indicates that the glutamate EC_{50}s for 9a + 9b and 9a + 9c are significantly different to 9b + 9c, but not to 9a + 9b + 9c (alpha = 0.05).
[b] Indicates the abamectin EC_{50}s for 9c is significantly different to 9a, but not to 9b (alpha = 0.05).

change range among the four EC_{50}s was no more than 1.8-fold. No significant change in the EC_{50}s and nHs among oocytes co-injected with different PxGluCls variant cRNAs were observed ($p > 0.05$), suggesting oocytes co-expressed two or three variants showed a similar response to abamectin.

3.4. Sensitivity of PxGluCl splice variants to fipronil

Fipronil, a ligand-gated chloride channels blocker with insecticidal potency, was used to test whether alternative splicing produces differences in the pharmacological properties of PxGluCls. The perfusion of fipronil reduced glutamate-induced inwards currents (see the sample traces in Fig. 4A). The C-R curves of fipronil for 9a, 9b and 9c channels gave IC_{50}s of 10.22 ± 4.08 μM, 3.79 ± 2.02 μM, and 12.92 ± 7.65 μM, respectively (Table 2, Fig. 4B). The 9b channels were more sensitive to this compound than 9a channels (unpaired *t*-test, t = 1.764 df = 8, $p = 0.1158$) and 9c channels (unpaired *t*-test with Welch's correction, t = 1.924 df = 4, $p = 0.1266$), with 2.7- and 3.4-fold reduction in IC_{50}s.

The IC_{50}s of fipronil for PxGluCls composed of different variants were 55.45 ± 19.48 μM for 9a + 9b, 32.67 ± 21.09 μM for 9a + 9c, 16.47 ± 6.92 μM for 9b + 9c and 57.99 ± 14.55 μM for 9a + 9b + 9c (Table 2, Fig. 4C). Inhibition by fipronil was not significantly different among the four co-expressed channels ($p > 0.05$). Interestingly, the potencies of fipronil to the heteromeric expressed PxGluCls were lower than that of the homomeric-expressed PxGluCls to some extent (Table 2).

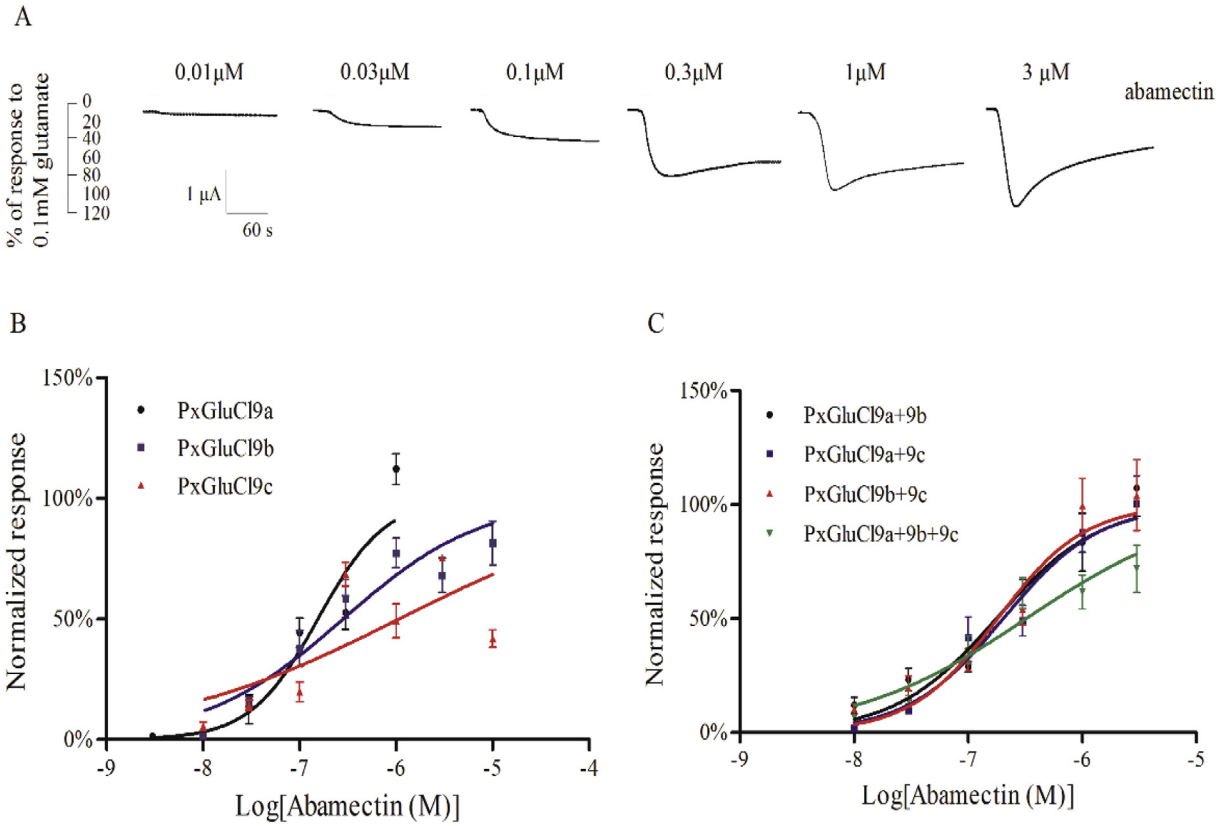

Fig. 3. Abamectin responses of *PxGluCls* containing variant subunits singly or co-expressed in *Xenopus* oocytes. (A) Representative current traces induced by abamectin from 0.01 μM to 3 μM in channels containing singly expressed 9a variant. (B) Abamectin concentration response curves obtained for singly expressed variants. (C) Abamectin concentration response curves obtained for co-expressed variants. Data are the mean ± SEM from n = 4–7 oocytes from 2 to 3 different frogs.

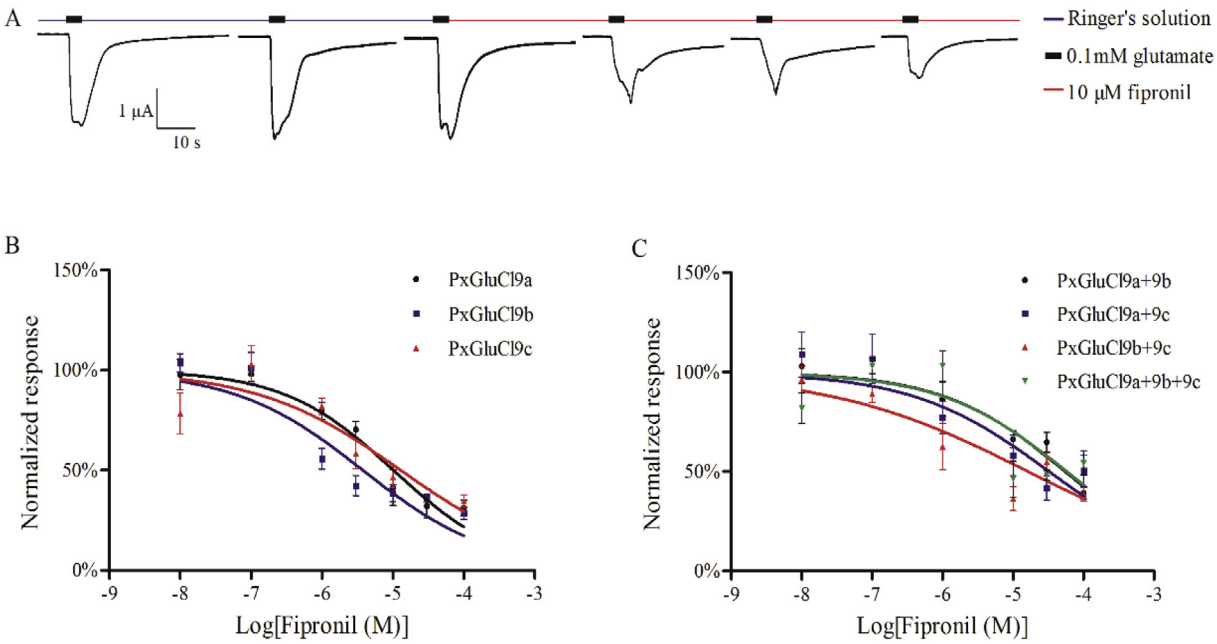

Fig. 4. Fipronil inhibition of glutamate-induced responses of *PxGluCls* containing variant subunits singly or co-expressed in *Xenopus* oocytes. (A) Representative current traces showing the effect of 10 μM fipronil on the 0.1 mM glutamate response in channels containing singly expressed 9a variant. (B) Fipronil concentration response curves obtained for singly expressed variants. (C) Fipronil concentration response curves obtained for co-expressed variants. Data are the mean ± SEM from n = 4–6 oocytes from 2 to 3 different frogs.

4. Discussion

Field populations of the *P. xylostella* pest have evolved various levels of resistance to 95 active ingredients (APRD, 2018), including abamectin (Pu et al., 2010) and fipronil (Wang et al., 2016b) pesticides that act on GluCls. We previously identified three mutually exclusive splice variants of *P. xylostella* GluCl exon 3 (Wang et al., 2016a) and in this current study we focused on exon 9 splice variants. We show that 9a, 9b and 9c variants expressed individually or co-expressed in oocytes produce robust inward currents in a dose-dependent pattern in response to glutamate. In addition, abamectin or fipronil either induced or inhibited inward currents, respectively, and there was a significant difference in GluCl sensitivity to these compounds depending on the expressed exon 9 variant.

Resistance to avermectins has been associated with point mutations of GluCls in *C. elegans*, *D. melanogaster*, *T. urticae* and *P. xylostella* (Dent et al., 2000; Dermauw et al., 2012; Kane et al., 2000; Kwon et al., 2010; Wang et al., 2016a, 2017). Our electrophysiological study found a 8.2-fold reduction in abamectin sensitivity with the exon 9c 12-aa deletion isoform when compared to 9a, which is the most common type of PxGluCl (described in Wang et al., 2016a and Wang et al., 2017). In addition, the exon 9b 9-aa deletion of PxGluCl also reduced the sensitivity to abamectin by 2.2-fold compared with 9a. Another study of *P. xylostella* (Liu et al., 2014) found that the expression of exon 9c produced a shift in the EC_{50} of abamectin from 118 nM to 1146 nM, which was about 10-fold higher than that of wild type channels. In contrast, with *B. mori* a partial deletion of exon 9 named 9pΔ (corresponding to the exon 9c of PxGluCl) had almost no impact on ivermectin action (Furutani et al., 2014).

The inhibitory potencies of fipronil differed among the three variants, with 9b showing more sensitivity (2.7- to 3.4-fold) than 9a or 9c isoforms. Furthermore, all heteromeric channels showed lower sensitivity to fipronil than homomeric channels. We found that fipronil inhibited glutamate-induced currents in PxGluCls with micromolar IC_{50}s (Table 2). These IC_{50}s values are significantly higher than found with other insects and nemotodes, where IC_{50}s range from 10 nM to 2930 nM with the exception of *C. elegans* glc-3 (IC_{50} of 11.5 μM). These findings suggest that substantial variations in sensitivity to fipronil can occur between different species. Although PxGluCls are considered the secondary target of fipronil after GABACls, it is possible that the upregulated constitutive expression of 9a, 9c or heteromeric channels may enhance synergistic resistance to fipronil in the field.

The individual 9a, 9b and 9c splice variants appear to have a similar sensitivity towards glutamate as we found no significant difference in the EC_{50}s and nHs between homomeric channels. Similarly in *L. striatellus* there were no significant differences in the response of LsGluCl-AL (a 21-bp stretch observed immediately downstream of intron 8) channel to glutamate, when compared with the LsGluCl-AS (the normal sequence) channel (Wu et al., 2017). However, other studies did find differences in glutamate sensitivity depending on the exon 9 transcript. With the *B. mori* GluCl the 9pΔ deletion (corresponding to PxGluCl exon 9c) had a small effect on glutamate action (Furutani et al., 2014). An even greater difference was found in an earlier study of *P. xylostella* GluCl where exon 9c variant was found to be about 13-fold less sensitive to glutamate compared to the wild-type (exon 9a) receptor (Liu et al., 2014).

The intracellular domain remains the most poorly characterized region of LGIC receptors. Only the structures of acetylcholine and serotonin receptors have part of their TM3-TM4 linkers resolved (Unwin, 2005; Basak et al., 2018). These structures have an alpha-helical region of about 20 residues termed the 'MA' helix that precedes TM4 and extends into the cytoplasm where MAs meet to form a pentameric helix bundle. Although this structural feature may be conserved in GluCl receptors, the region encoded by the exon 9 variants is further than 20 residues from TM4 and is therefore predicted to lie just beyond the putative MA helix. We speculate that variation in this region may affect inter-monomer packing by the MA helices. As each MA helix is contiguous with TM4, a change in MA packing could be propagated via contact with TM4 to effect the conformation of the transmembrane domain and reposition residues that are ligand-binding determinants. Therefore an allosteric modification of the avermectin and fipronil binding sites may explain the effect of splice variants on GluCl sensitivity towards these two compounds. The structural effects exerted by the splice variants may not be propagated as far as the extracellular

domain, which could account for the similar glutamate sensitivity of all the GluCls investigated in our study. However, a previous study with PxGluGl exon 9a and 9c variants did find a significant difference in glutamate sensitivity (Liu et al., 2014), which suggests the involvement of another mechanism. It is possible that post-translational modifications mediated by the TM3-TM4 linker can effect GluCl glutamate sensitivity. We note that the TM3-TM4 linkers of nAChR and 5-HT3A receptors provide sites for post-translational modifications, which may affect channel trafficking, kinetics and desensitization (McKinnon et al., 2012; Tsetlin et al., 2011).

In summary, we functionally characterized and determined pharmacological properties of a complete set of alternative PxGluCl exon 9 splices and our results provide evidence that an as yet uncharacterized region of LGICs can have an impact on receptor pharmacology. We found that the shortest variant 9c is associated with a decreased sensitive to abamectin whereas homomers formed from the medium-length 9b variant are more sensitive to fipronil. The physiological roles of the different homomeric and heteromeric assembled channels remain to be examined but our study indicates that monitoring the frequency of the splice variants may provide a valuable molecular approach to evaluating the development of abamectin and fipronil resistance in the field.

Acknowledgements

This work was supported by grants from National Natural Science Foundation of China (31772196 and 31301693), the Chinese Ministry of Agriculture (the 948 project no. 2014-S10). Rothamsted Research also receives grant-aided support from the UK Biotechnology and Biological Sciences Research Council (BBSRC).

Appendix A. Supplementary data

Supplementary data to this article can be found online at https://doi.org/10.1016/j.ibmb.2018.12.005.

References

APRD, 2018. Arthropod Pesticide Resistance Database. http://www.pesticideresistance.org/, Accessed date: 5 March 2018.

Basak, S., Gicheru, Y., Samanta, A., Molugu, S.K., Huang, W., Fuente, M. la de, Hughes, T., Taylor, D.J., Nieman, M.T., Moiseenkova-Bell, V., Chakrapani, S., 2018. Cryo-EM structure of 5-HT3A receptor in its resting conformation. Nat. Commun. 9, 514.

Buckingham, S.D., Biggin, P.C., Sattelle, B.M., Brown, L.A., Sattelle, D.B., 2005. Insect GABA receptors: splicing, editing, and targeting by antiparasitics and insecticides. Mol. Pharmacol. 68, 942–951.

Cull-Candy, S.G., 1976. Two types of extrajunctional L-glutamate receptors in locust muscle fibres. J. Physiol. 255, 449–464.

Dent, J.A., Smith, M.M., Vassilatis, D.K., Avery, L., 2000. The genetics of ivermectin resistance in *Caenorhabditis elegans*. Proc. Natl. Acad. Sci. U. S. A. 97, 2674–2679.

Dermauw, W., Ilias, A., Riga, M., Tsagkarakou, A., Grbic, M., Tirry, L., Van Leeuwen, T., Vontas, J., 2012. The cys-loop ligand-gated ion channel gene family of *Tetranychus urticae*: implications for acaricide toxicology and a novel mutation associated with abamectin resistance. Insect Biochem. Mol. Biol. 42, 455–465.

Furutani, S., Ihara, M., Nishino, Y., Akaike, A., Jones, A.K., Sattelle, D.B., Matsuda, K., 2014. Exon 3 splicing and mutagenesis identify residues influencing cell surface density of heterologously expressed silkworm (*Bombyx mori*) glutamate-gated chloride channels. Mol. Pharmacol. 86, 686–695.

Fuse, T., Kita, T., Nakata, Y., Ozoe, F., Ozoe, Y., 2016. Electrophysiological characterization of ivermectin triple actions on *Musca* chloride channels gated by L-glutamic acid and gamma-aminobutyric acid. Insect Biochem. Mol. Biol. 77, 78–86.

Jones, A.K., Sattelle, D.B., 2006. The cys-loop ligand-gated ion channel superfamily of the honeybee, *Apis mellifera*. Invertebr. Neurosci. 6, 123–132.

Jones, A.K., Sattelle, D.B., 2007. The cys-loop ligand-gated ion channel gene superfamily of the red flour beetle, *Tribolium castaneum*. BMC Genomics 8, 327.

Jones, A.K., Sattelle, D.B., 2008. The cys-loop ligand-gated ion channel gene superfamily of the nematode, *Caenorhabditis elegans*. Invert. Neurosci. 8, 41–47.

Jones, A.K., Bera, A.N., Lees, K., Sattelle, D.B., 2010. The cys-loop ligand-gated ion channel gene superfamily of the parasitoid wasp, *Nasonia vitripennis*. Heredity 104, 247–259.

Kane, N.S., Hirschberg, B., Qian, S., Hunt, D., Thomas, B., Brochu, R., Ludmerer, S.W., Zheng, Y., Smith, M., Arena, J.P., Cohen, C.J., Schmatz, D., Warmke, J., Cully, D.F., 2000. Drug-resistant *Drosophila* indicate glutamate-gated chloride channels are targets for the antiparasitics nodulisporic acid and ivermectin. Proc. Natl. Acad. Sci. U. S. A. 97, 13949–13954.

Kita, T., Ozoe, F., Ozoe, Y., 2014. Expression pattern and function of alternative splice variants of glutamate-gated chloride channel in the housefly *Musca domestica*. Insect Biochem. Mol. Biol. 45, 1–10.

Kwon, D.H., Yoon, K.S., Clark, J.M., Lee, S.H., 2010. A point mutation in a glutamate-gated chloride channel confers abamectin resistance in the two-spotted spider mite, *Tetranychus urticae* Koch. Insect Mol. Biol. 19, 583–591.

Liu, F., Shi, X.Z., Liang, Y.P., Wu, Q.J., Xu, B.Y., Xie, W., Wang, S.L., Zhang, Y.J., Liu, N.N., 2014. A 36-bp deletion in the alpha subunit of glutamate-gated chloride channel contributes to abamectin resistance in *Plutella xylostella*. Entomol. Exp. Appl. 153, 85–92.

McKinnon, N.K., Bali, M., Akabas, M.H., 2012. Length and amino acid sequence of peptides substituted for the 5-HT3A receptor M3-M4 loop may affect channel expression and desensitization. PLoS One 7, e35563.

Meyers, J.I., Gray, M., Kuklinski, W., Johnson, L.B., Snow, C.D., Black, W.C., Partin, K.M., Foy, B.D., 2015. Characterization of the target of ivermectin, the glutamate-gated chloride channel, from *Anopheles gambiae*. J. Exp. Biol. 218, 1478–1486.

Narahashi, T., Zhao, X., Ikeda, T., Salgado, V.L., Yeh, J.Z., 2010. Glutamate-activated chloride channels: unique fipronil targets present in insects but not in mammals. Pestic. Biochem. Physiol. 97, 149–152.

Pu, X., Yang, Y.H., Wu, S.W., Wu, Y.D., 2010. Characterisation of abamectin resistance in a field-evolved multiresistant population of *Plutella xylostella*. Pest Manag. Sci. 66, 371–378.

Semenov, E.P., Pak, W.L., 1999. Diversification of *Drosophila* chloride channel gene by multiple posttranscriptional mRNA modifications. J. Neurochem. 72, 66–72.

Tsetlin, V., Kuzmin, D., Kasheverov, I., 2011. Assembly of nicotinic and other Cys-loop receptors. J. Neurochem. 116, 734–741.

Unwin, N., 2005. Refined structure of the nicotinic acetylcholine receptor at 4 Å resolution. J. Mol. Biol. 346, 967–989.

Wang, X., Wang, R., Yang, Y., Wu, S., O'Reilly, A.O., Wu, Y., 2016a. A point mutation in the glutamate-gated chloride channel of *Plutella xylostella* is associated with resistance to abamectin. Insect Mol. Biol. 25, 116–125.

Wang, X.L., Wu, S.W., Gao, W.Y., Wu, Y.D., 2016b. Dominant inheritance of field-evolved resistance to fipronil in *Plutella xylostella* (Lepidoptera: Plutellidae). J. Econ. Entomol. 109, 334–338.

Wang, X.L., Puinean, A.M., O'Reilly, A.O., Williamson, M.S., Smelt, C.L.C., Millar, N.S., Wu, Y.D., 2017. Mutations on M3 helix of *Plutella xylostella* glutamate-gated chloride channel confer unequal resistance to abamectin by two different mechanisms. Insect Biochem. Mol. Biol. 86, 50–57.

Wolstenholme, A.J., 2010. Recent progress in understanding the interaction between avermectins and ligand-gated ion channels: putting the pests to sleep. Invertebr. Neurosci. 10, 5–10.

Wolstenholme, A.J., 2012. Glutamate-gated chloride channels. J. Biol. Chem. 287, 40232–40238.

Wu, S.F., Mu, X.C., Dong, Y.X., Wang, L.X., Wei, Q., Gao, C.F., 2017. Expression pattern and pharmacological characterisation of two novel alternative splice variants of the glutamate-gated chloride channel in the small brown planthopper *Laodelphax striatellus*. Pest Manag. Sci. 73, 590–597.

Zhao, X.L., Yeh, J.Z., Salgado, V.L., Narahashi, T., 2004. Fipronil is a potent open channel blocker of glutamate-activated chloride channels in cockroach neurons. J. Pharmacol. Exp. Therapeut. 310, 192–201.